Joint Localization and Clock Offset Estimation via time-of-arrival with ranging offset

Ido Nevat[1], François Septier[2], Karin Avnit[3], Gareth W. Peters [4], and Laurent Clavier [5]
[1] TUMCREATE, Singapore.
[2] Institut Mines-Télécom / Télécom Lille/CRIStAL UMR CNRS 9189, Villeneuve dascq, France.
[3] Singapore Institute of Technology (SIT), Singapore.
[4] Department of Statistical Sciences, University College London (UCL), England.
[5] Institut Mines-Télécom, Télécom Lille, IEMN, UMR CNRS 8520 .

***Abstract*—We develop a novel algorithm for Geo-Spatial location estimation for Internet of Things (IoT) networks by utilizing a One-Way Time-of-Arrival (OW-TOA) technology. Although very popular, OW-TOA based localization techniques are negatively affected by three phenomena: i) wireless connectivity between the target and the receiving nodes is not guaranteed (audibility), resulting in likelihood surface which may produce a non-unique maxima; ii) clock offset imperfection which is a result of a fixed deviation from a reference clock; and iii) a ranging offset which introduces distance dependent bias to the OW-TOA measurements. We develop a new statistical framework which incorporates these aspects and then derive the *joint localization and clock offset* Maximum Likelihood Estimator to jointly estimate the location of the target and the clock offset. To solve the resulting non-convex optimization problem we propose to use the Cross-Entropy method.**

I. Introduction

The term "Internet-of-Things" (IoT) describes several technologies and research disciplines in which the Internet extends into the physical world [1]–[4]. For the IoT paradigm to be successful it will need to be able to track the location (and the movement) that comprise the local instantiation of the IoT at any given time and place of these objects, thus providing location-based services, which we denote as Location of Things (LoT). One promising approach that aims at achieving sub-centimeter accuracy is based on Ultra-Wideband (UWB) ranging [5]–[8]. The process of ranging involves estimation of the distance between any two nodes. There are several techniques available for ranging such as Angle of Arrival (AOA), Received Signal Strength (RSS), Time of Arrival (ToA), and a combination of these [9].

We present a new statistical framework for Geo-Spatial location estimation for Internet of Things (IoT) networks by utilizing a One-Way Time-of-Arrival (OW-TOA) technology, which exploits the fine delay resolution property of wideband signals and have great potential for providing sub-centimeter resolution [6]–[8]. OW-TOA is a very popular method to estimate the point-to-point distance between two communicating devices. This is achieved based on the measurements of the time that a signal is required to travel from one device to the other. An example of the OW-TOA protocol can be found in [10] which aims at reducing the communication load and explores the broadcast property of WSN. However, OW-TOA based localization techniques are negatively affected by the following phenomena:

1) **Audibility** of the receiving nodes is not guaranteed, resulting in likelihood surface which have non-unique maxima (ambiguity phenomenon). This degrades the localization performance [11]–[14].
2) **Clock offset** imperfection manifested by a fixed deviation from a reference clock at time zero [15].
3) **Ranging offset** which introduces distance dependent bias to the OW-TOA measurements, due to variations in the received signal strength [16], [17].

To tackle these three important aspects in a holistic way, we develop a novel statistical model which incorporates all these aspects. This results in a statistical dependence between the ranging offset and audibility information which was not exploited before, and results in a likelihood structure which contains truncated distributions. We then formulate and develop the *joint localization and clock offset* algorithm to estimate both the location of the target and the clock offset. We evaluate the estimation performance of the proposed algorithm via simulations. We therefore summarize our contributions as follows:

1) We extend current OW-TOA based models and incorporate the ranging offset due to RSS variations;
2) We show that the inclusion of the ranging offset in the statistical model involves working with truncated Normal distributions. We prove that this inclusion still results in an analytic expression for the likelihood function.
3) We derive the Joint Maximum Likelihood Estimator (MLE) for the location of the node and the clock offset. We solve the optimization problem via the Cross Entropy method.

ISBN 978-90-827970-1-5 © EURASIP 2018

II. Wireless Sensor Network System Model

We consider a network with N Base Stations (BS) whose locations are known and one target node at an unknown location to be estimated. We now present the system model:

1) A single target is located at unknown location $\theta = [x_u \;\; y_u] \in \chi \subseteq \mathbb{R}^2$.
2) Assume N Base Stations (BS) deployed in a 2-D plane, where the known location of the n-th BS is $\mathbf{x}_n = [x_n \;\; y_n] \in \chi$.
3) The target transmits a signal with power P_t while the N BS listen to the ranging packets and record timestamps locally. The trip time, $t_{\text{rt}}(A,B)$, measured at BS A located at $\Theta_A = [x_a \;\; y_a]$ from target B located at $\Theta_B = [x_b \;\; y_b]$ is given by

$$t_{\text{rt}}(A,B) = t_{\text{stop}} - t_{\text{start}} + t_\delta + T_\psi\left(P^{\text{R}}(\theta_A,\theta_B)\right) + T_p, \quad (1)$$

where t_{start} is the transmitted time stamp at node B, t_{stop} is the received time stamp at node A, t_δ is the common clock offset [15], $T_\psi\left(P^{\text{R}}(\theta_A,\theta_B)\right)$ is the random ranging offset due to the received power [16], [17], T_p is the random offset time accounting for all processing delays in the system, which include the time for Node B to transmit the packet, and the time taken to Node A to process the packet.

4) **Audibility model:** in order to obtain ranging measurements between two devices in the sensor network, the two devices need to be connected so that they can exchange messages. Due to various physical phenomena such as fading and multi-path, a simple deterministic communication model, such as the disk model, may not be well suited to describe the stochastic nature of the wireless channel. To address this issue, we adopt a random connection model which encodes random environmental parameters such as path loss. We express the notion of audibility via Power Loss Model, which is based on an inverse power law model of the attenuation, and a *log*-normal shadow fading. The received power by node located at θ_A from a transmitting target at θ_B is given by:

$$P^{\text{R}}(\theta_A,\theta_B) = p^{\text{T}} - 10\alpha\log\frac{d(\theta_A,\theta_B)}{d_0} + W \quad [\text{dB}],$$

and p^{T} is the transmitted power by the target B, α is the path-loss exponent, $d(\theta_A,\theta_B) := \sqrt{(x_a-x_b)^2+(y_a-y_b)^2}$ is the Euclidean distance between the target A and BS B, d_0 is a reference distance, and W represents the shadowing effect, modelled as a Normal random variable, i.e. $W \sim \mathcal{N}(\mu_w,\sigma_w^2)$. Let $\mathbf{\Gamma} \in \{0,1\}^N$ be the binary indicator vector which indicates which BS successfully received the message from the target, where Γ_n specifies if the target is audible by the n-th BS , meaning that

$$\begin{cases}\Gamma_n = 1, \text{ if } P^{\text{R}}(\mathbf{x}_n,\theta) > \lambda,\\ \Gamma_n = 0, \text{ Otherwise}\end{cases}$$

where $P^{\text{R}}(\mathbf{x}_n,\theta)$ is the received power at the n-th BS from the target. Also, λ is a pre-defined threshold representing the receiver's sensitivity.

5) **Ranging model:** let $\mathbf{y} \in \mathbb{R}^N$ be the observation vector, and the ranging measurement at the n-th BS is given by multiplying the trip time $t_{\text{rt}}(A,B)$ given in (1), by the speed of light:

$$y_n = \begin{cases} d(\mathbf{x}_n,\theta) + \delta + \Psi_n\left(P^{\text{R}}(\mathbf{x}_n,\theta)\right) + E_n^{\text{r}}, \\ \quad \text{if } \Gamma_n = 1 \text{ (Audible node)} \\ \varnothing, \text{Otherwise (Inaudible node)}\end{cases}$$

where $\varnothing$ denotes "no observation", $\delta \in \xi$ is the unknown *common clock offset distance*, $\Psi_n\left(P^{\text{R}}(\mathbf{x}_n,\theta)\right) \sim \mathcal{N}\left(\mu_\Psi(\mathbf{x}_n,\theta),\sigma_\Psi^2\right)$ is the n-th *ranging offset* and $E_n^{\text{r}} \sim \mathcal{N}(\mu_r,\sigma_r^2)$ is the *ranging error*.

6) The ranging offset $\Psi\left(P^{\text{R}}(\theta_A,\theta_B)\right)$ is given by a simple linear regression model which we fit via measurements and is given by:

$$\Psi\left(P^{\text{R}}(\theta_A,\theta_B)\right) = \beta_1 P^{\text{R}}(\theta_A,\theta_B) + \beta_0 + E^{\text{reg}}$$

where β_0,β_1 are the covariates, and E^{reg} is the error term modelled as $E^{\text{reg}} \sim \mathcal{N}\left(0,\sigma^2_{E^{\text{reg}}}\right)$. The model parameters $\beta_0,\beta_1,\sigma^2_{E^{\text{reg}}}$ are calibrated via Maximum Likelihood Estimator (MLE) from the data-set [17]. It follows that in the ranging distance offset is given by:

$$\Psi\left(P^{\text{R}}(\theta_A,\theta_B)\,|\beta_0,\beta_1,\sigma^2_{E^{\text{reg}}}\right) \sim \mathcal{N}\left(\mu_\Psi(\theta_A,\theta_B),\sigma_\Psi^2\right),$$

where $\mu_\Psi(\theta_A,\theta_B) = \beta_1\left(p^{\text{T}} - 10\alpha\log\frac{d(\theta_A,\theta_B)}{d_0}\right) + \beta_0$, and $\sigma_\Psi^2 = \beta_1^2\sigma_W^2 + \sigma^2_{E^{\text{reg}}}$.

III. Joint Location and Clock Offset Estimation

We now formulate the joint MLE for the unknown location of the target, θ, and the clock offset δ, given set of ranging observations $y_{1:N}$, and and audibility indicators $\Gamma_{1:N}$. The joint MLE is given by:

$$\begin{aligned}\left(\widehat{\theta},\widehat{\delta}\right) &= \underset{\theta\in\chi,\delta\in\xi}{\arg\max}\, p(y_{1:N},\Gamma_{1:N}|\theta,\delta)\\ &= \underset{\theta\in\chi,\delta\in\xi}{\arg\max}\, p(y_{1:N}|\Gamma_{1:N},\theta,\delta)\,\Pr(\Gamma_{1:N}|\theta)\\ &= \underset{\theta\in\chi,\delta\in\xi}{\arg\max} \sum_{n=1}^{N}\log p(y_n|\Gamma_n=1,\theta,\delta)\,\mathbb{1}(\Gamma_n=1)\\ &\qquad + \sum_{n=1}^{N}\log\Pr(\Gamma_n=1|\theta)\,\mathbb{1}(\Gamma_n=1)\\ &\qquad + \sum_{n=1}^{N}\log\Pr(\Gamma_n=0|\theta)\,\mathbb{1}(\Gamma_n=0).\end{aligned} \quad (2)$$

ISBN 978-90-827970-1-5 © EURASIP 2018

Next, in Lemma 1 and Lemma 2 we present the likelihood function components $p\left(y_n|\Gamma_n=1,\theta,\delta\right)$, $\Pr\left(\Gamma_n=1|\theta\right)$ and $\Pr\left(\Gamma_n=0|\theta\right)$.

Lemma 1 (Ranging component likelihood function of an audible node $p\left(y_n|\Gamma_n=1,\theta,\delta\right)$)**.**
The likelihood function of the n-th audible node is:

$$p\left(y_n|\Gamma_n=1,\theta,\delta\right)=\frac{\exp\left(-\frac{\left(d(\mathbf{x}_n,\theta)+\delta+\mu_\Psi(\mathbf{x}_n,\theta)-y_n\right)^2}{2\left(\sigma_\Psi^2+\sigma_\epsilon^2\right)}\right)}{\sqrt{2\pi}\left(\mathrm{erf}\left[\frac{\Lambda-\mu_\Psi(\mathbf{x}_n,\theta)}{\sqrt{2}\sigma_\Psi}\right]+1\right)\sqrt{\sigma_\Psi^2+\sigma_\epsilon^2}}$$
$$\times\left(\mathrm{erf}\left[\frac{\left(\Lambda-y_n+d\left(\mathbf{x}_n,\theta\right)+\delta\right)\sigma_\Psi^2+\left(\Lambda-\mu_\Psi\left(\mathbf{x}_n,\theta\right)\right)\sigma_\epsilon^2}{\sqrt{2}\sigma_\Psi\sigma_\epsilon\sqrt{\sigma_\Psi^2+\sigma_\epsilon^2}}\right]+1\right)$$

Proof. See Appendix A □

Lemma 2 (Audibility component likelihood function $\Pr\left(\Gamma_n|\mathbf{x}_n,\theta\right)$)**.**
The audibility likelihood function of the the n-th node is:

$$Pr\left(\Gamma_n|\mathbf{x}_n,\theta\right)=\begin{cases}\frac{1}{2}-\frac{1}{2}erf\left[\frac{\lambda-\left(p^T-10\alpha\log\frac{d(\mathbf{x}_n,\theta)}{d_0}\right)}{\sqrt{2\sigma_W^2}}\right], & \Gamma_n=1\\ \frac{1}{2}+\frac{1}{2}erf\left[\frac{\lambda-\left(p^T-10\alpha\log\frac{d(\mathbf{x}_n,\theta)}{d_0}\right)}{\sqrt{2\sigma_W^2}}\right], & \Gamma_n=0.\end{cases}$$

Proof. See Appendix B □

By plugging the results of Lemma 1 and Lemma 2 into the MLE in Eq. (2), we obtain the joint location and clock offset maximum likelihood estimator, presented in the following:

Proposition 1. *The joint location and clock offset Maximum Likelihood estimator is given by the solution to the following optimization problem:*

$$\left(\widehat{\theta},\widehat{\delta}\right)=\underset{\theta\in\chi,\delta\in\xi}{\arg\max}\sum_{n=1}^{N}\Bigg\{-\frac{\left(d\left(\mathbf{x}_n,\theta\right)+\delta+\mu_\Psi\left(\mathbf{x}_n,\theta\right)-y_n\right)^2}{2\left(\sigma_\Psi^2+\sigma_\epsilon^2\right)}$$
$$+\log\left(\mathrm{erf}\left[\frac{\left(\Lambda-y_n+d\left(\mathbf{x}_n,\theta\right)+\delta\right)\sigma_\Psi^2+\left(\Lambda-\mu_\Psi\left(\mathbf{x}_n,\theta\right)\right)\sigma_\epsilon^2}{\sqrt{2}\sigma_\Psi\sigma_\epsilon\sqrt{\sigma_\Psi^2+\sigma_\epsilon^2}}\right]+1\right)$$
$$-\log\left(\mathrm{erf}\left[\frac{\Lambda-\mu_\Psi\left(\mathbf{x}_n,\theta\right)}{\sqrt{2}\sigma_\Psi}\right]+1\right)\Bigg\}\mathbb{1}\left(\Gamma_n=1\right)$$
$$+\log\left(1-\mathrm{erf}\left[\frac{\lambda-\left(p^{\mathrm{T}}-10\alpha\log\frac{d(\mathbf{x}_n,\theta)}{d_0}\right)}{\sqrt{2\sigma_W^2}}\right]\right)\mathbb{1}\left(\Gamma_n=1\right)$$
$$+\log\left(1+\mathrm{erf}\left[\frac{\lambda-\left(p^{\mathrm{T}}-10\alpha\log\frac{d(\mathbf{x}_n,\theta)}{d_0}\right)}{\sqrt{2\sigma_W^2}}\right]\right)\mathbb{1}\left(\Gamma_n=0\right).$$

IV. Algorithm implementation via Cross Entropy method

Calculating the joint MLE involves solving a trivariate optimization problem, where the objective function is non-convex and non-linear in θ and δ. To solve this optimization problem, we develop an efficient Monte Carlo stochastic optimization algorithm, which is based on the Cross Entropy Method (CEM) [18]. To implement the CEM, the sampling pdf $h\left(\cdot;\mathbf{v}\in\mathcal{V}\right)$ needs to be specified, as well as solving the stochastic optimization problem to update the parameter vector $\mathbf{v}$:

$$\mathbf{v}_t=\underset{\mathbf{v}}{\arg\max}\,\frac{1}{J}\sum_{i=1}^{J}\mathbb{1}\left(U\left(\mathbf{z}^{(i)}\right)\geq\gamma_t\right)\ln h\left(\mathbf{z}^{(i)};\mathbf{v}\right),$$

where $\mathbf{z}:=\left(\left[x_u\ ,y_u\right],\delta\right)$, $U\left(\mathbf{z}\right)$ as the objective function in Proposition 1, and γ_t is a quantile-based threshold. We choose the sampling density to be independent Normal distribution. This choice is motivated by the availability of fast and exact normal random number generators and the fact that the solution for the stochastic optimization problem yields a simple analytic solution. Our sampling density is given by:

$$h\left(\cdot;\mathbf{v}\in\mathcal{V}\right)^{:}=\mathcal{N}\left(x_u;\mu_x,\sigma_x^2\right)\mathcal{N}\left(y_u;\mu_y,\sigma_y^2\right)\mathcal{N}\left(\delta;\mu_\delta,\sigma_\delta^2\right),$$

where $\mathbf{v}:=\left[\mu_x,\sigma_x^2,\mu_y,\sigma_y^2,\mu_\delta,\sigma_\delta^2\right]$. Based on this choice, the solution for the stochastic optimization problem is:

$$\mathbf{v}_t=\underset{\mathbf{v}_t}{\arg\max}\,\frac{1}{J}\sum_{i=1}^{J}\mathbb{1}\left(U\left(\mathbf{z}^{(i)}\right)\geq\widehat{\gamma}_t\right)$$
$$\times\left(\log\mathcal{N}\left(x_u;\mu_x,\sigma_x^2\right)+\log\mathcal{N}\left(y_u;\mu_y,\sigma_y^2\right)+\log\mathcal{N}\left(\delta;\mu_\delta,\sigma_\delta^2\right)\right).$$

Solving this optimization problem results in an analytic form for the new set of values for $\mathbf{v}_t$. For example, the two model parameters related with $\mathbf{x}_u$, given by μ_x,σ_x^2, are updated as follows:

$$\mu_x=\frac{\sum_{i=1}^{J}\mathbb{1}\left(U\left(\mathbf{z}^{(i)}\right)\geq\widehat{\gamma}_t\right)\theta_x^{(i)}}{\sum_{i=1}^{J}\mathbb{1}\left(U\left(\mathbf{z}^{(i)}\right)\geq\widehat{\gamma}_t\right)},$$
$$\sigma_x^2=\frac{\sum_{i=1}^{J}\mathbb{1}\left(U\left(\mathbf{z}^{(i)}\right)\geq\widehat{\gamma}_t\right)\left(\mu_x-\theta_x^{(i)}\right)^2}{\sum_{i=1}^{J}\mathbb{1}\left(U\left(\mathbf{z}^{(i)}\right)\geq\widehat{\gamma}_t\right)}. \tag{3}$$

The parameter values for y_u and δ can be found in a similar way. Lastly, the smoothing matrix Σ is chosen to be a diagonal matrix with values $\alpha_x,\alpha_y,\alpha_\delta$, which are typically in the range $0.6-0.9$.

V. Simulation results

We now present numerical simulations to evaluate the performance of the joint MLE for various parameters. We consider an open environment of size 10×10 meters with a line-of-sight, and four BSs located at each of the corners of the room.

A. Convergence of the Cross Entropy method

We present results which show how the convergence of the CE based algorithm. We consider the case where the target is located at $\{x=5,y=5\}$ and the clock offset $\delta=3$. We then run 200 realizations from the model where for each realization the starting point of the

ISBN 978-90-827970-1-5 © EURASIP 2018

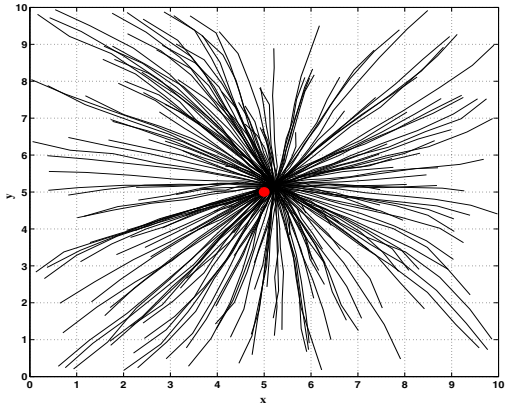

Fig. 1: Cross Entropy algorithm convergence over 200 realizations. The true target location (marked in red) is $\{x = 5, y = 5\}$. Each line represents a single mean sample path of the Cross Entropy algorithm.

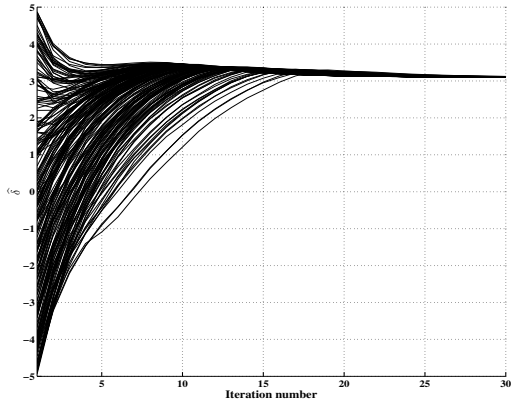

Fig. 2: Cross Entropy algorithm convergence over 200 realizations. The true clock offset is $\delta = 3$. Each line represents a single mean sample path of the Cross Entropy algorithm.

estimate location and clock offset is randomly chosen. The sample paths of the CE algorithm are presented in Figs. 1-2. We observe that in all cases the estimated parameters are close to the true values which demonstrates that the CE algorithm performs very well and does not seem to get trapped in a local maxima.

B. Joint estimation performance

We evaluate the estimation performance of our algorithm as a function of the ranging noise variance σ_r^2. We also compare our proposed algorithm with a brute-force 3-D search over a fine grid of Proposition 1. In addition, we also compare with a Naive approach which neglects to take into account both audibility and ranging offsets. The results are presented in Figs. 3-4 terms of Mean Squared Error (MSE). The two important concussions from these simulations are as follows:

1) The proposed algorithm performs very close to the brute-force approach. This demonstrates that the Cross-Entropy method based algorithm works very well and is able to locate the maxima of the objective function.
2) The proposed algorithm outperforms the Naive approach considerably. This shows the importance of utilising both audibility information as well as considering the ranging offset effect.

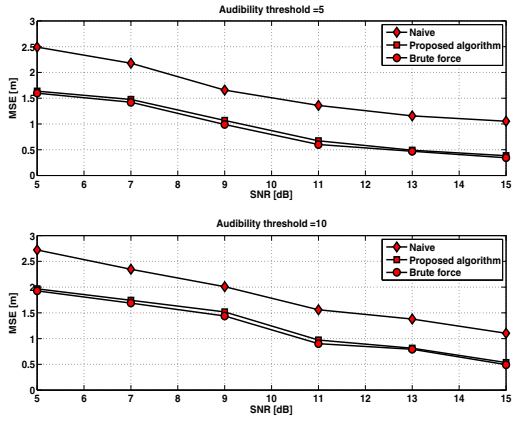

Fig. 3: Localization estimation performance

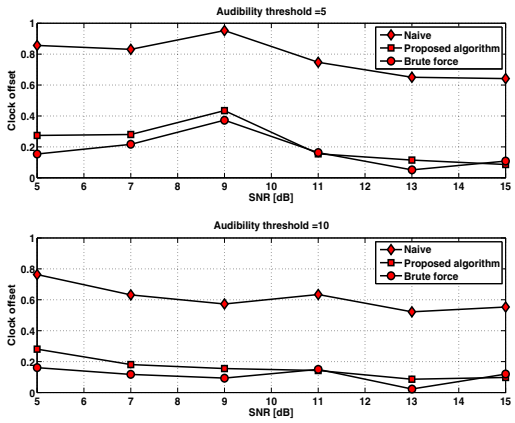

Fig. 4: Clock offset estimation performance

VI. ACKNOWLEDGMENTS

This work was financially supported by the Singapore National Research Foundation under its Campus for Research Excellence And Technological Enterprise (CREATE) program.

ISBN 978-90-827970-1-5 © EURASIP 2018

APPENDIX A
PROOF OF LEMMA 1

The ranging observation from the n-th audible node is given by:

$$\begin{aligned} y_n &= \mathrm{d}\left(\mathbf{x}_n,\theta\right)+\delta+\Psi_n\left(P^{\mathrm{R}}\left(\mathbf{x}_n,\theta\right)\right)+E_n^{\mathrm{r}} \\ &= \mathrm{d}\left(\mathbf{x}_n,\theta\right)+\delta+\beta_1\left(p^{\mathrm{T}}-10\alpha\log\frac{d\left(\theta,\mathbf{x}_n\right)}{d_0}+W_n\right)+\beta_0+E_n^{\mathrm{reg}}+E_n^{\mathrm{r}} \\ &= \underbrace{\mathrm{d}\left(\mathbf{x}_n,\theta\right)+\delta+\beta_0+E_n^{\mathrm{reg}}+E_n^{\mathrm{r}}}_{:=\widetilde{E}_n}+\beta_1\left(p^{\mathrm{T}}-10\alpha\log\frac{d\left(\theta,\mathbf{x}_n\right)}{d_0}+W_n\right) \\ &= \widetilde{E}_n+\beta_1 P^{\mathrm{R}}\left(\mathbf{x}_n,\theta\right). \end{aligned}$$

We now derive the distribution of $\widetilde{E}_n$ and $\beta_1 P^{\mathrm{R}}\left(\mathbf{x}_n,\theta\right)$, conditional on θ,δ.
First, the conditional distribution of $\widetilde{E}_n$ is given by

$$\widetilde{E}\left(n\right)|\theta,\delta\sim\mathcal{N}\left(\underbrace{d\left(\mathbf{x}_n,\theta\right)+\delta+\beta_0+\mu_r}_{\mu_{\widetilde{E}}},\underbrace{\sigma_r^2+\sigma_{E^{\mathrm{reg}}}^2}_{\sigma_{\widetilde{E}}^2}\right).$$

Next we derive the conditional distribution $\beta_1 P^{\mathrm{R}}\left(\mathbf{x}_n,\theta\right)|\Gamma_n=1,\theta$, while keeping in mind that the node is audible ($\Gamma_n=1$), meaning that $P^{\mathrm{R}}\left(\mathbf{x}_n,\theta\right)>\lambda$. Using the audibility definition, and remembering that $\beta_1<0$, we have that

$$\beta_1\left(p^{\mathrm{T}}-10\alpha\log\frac{d\left(\theta,\mathbf{x}_n\right)}{d_0}+W_n\right)\leq\underbrace{\beta_1\lambda}_{:=\Lambda}.$$

This means that $\beta_1\left(p^{\mathrm{T}}-10\alpha\log\frac{d(\theta,\mathbf{x}_n)}{d_0}+W_n\right)|\Gamma_n=1,\theta$ follows an *upper truncated Normal distribution*:

$$\begin{aligned} &\left(\beta_1\left(p^{\mathrm{T}}-10\alpha\log\frac{d\left(\theta,\mathbf{x}_n\right)}{d_0}+W_n\right)|\Gamma_n=1,\theta\right) \\ &\sim\mathcal{TN}\left(\underbrace{\beta_1\left(p^{\mathrm{T}}-10\alpha\log\frac{d\left(\theta,\mathbf{x}_n\right)}{d_0}+\mu_w\right)}_{\mu_n},\underbrace{\beta_1^2\sigma_w^2}_{\sigma_n^2},-\infty,\Lambda\right). \end{aligned}$$

We therefore obtain that $p\left(y_n|\Gamma_n=1,\theta\right)$ is given by the convolution of a Normal random variable $\left(\widetilde{E}\left(n\right)|\theta,\delta\sim\mathcal{N}\left(\mu_{\widetilde{E}},\sigma_{\widetilde{E}}^2\right)\right)$ and a truncated Normal random variable $\left(\beta_1 P^{\mathrm{R}}\left(\mathbf{x}_n,\theta\right)|\Gamma_n=1,\theta\sim\mathcal{TN}\left(\mu_n,\sigma_n^2,-\infty,\Lambda\right)\right)$. Using Lemma 1 we obtain the likelihood function in closed form as follows:

$$p\left(y_n|\Gamma_n=1,\theta,\delta\right)=f_{\mathrm{sum}}\left(y_n;\mu_{\widetilde{E}},\sigma_{\widetilde{E}}^2,\mu_n,\sigma_n^2,\Lambda\right).$$

APPENDIX B
PROOF OF LEMMA 2

We express the conditional audibility probability of the target node with the n-th node as follows:

$$\begin{aligned} \mathrm{P}r\left(\Gamma_n=1,|\mathbf{x}_n,\theta\right)&=\mathrm{P}r\left(P_T-10\alpha\log\frac{d\left(\mathbf{x}_n,\theta\right)}{d_0}+W>\lambda\right) \\ &=1-\frac{\mathrm{erf}\left[\frac{\lambda-\left(p^{\mathrm{T}}-10\alpha\log\frac{d(\mathbf{x}_n,\theta)}{d_0}\right)}{\sqrt{2\sigma_W^2}}\right]+1}{2} \end{aligned}$$

and since the event $\Gamma_i=0,|\mathbf{x}_n,\theta$ and $\Gamma_i=1,|\mathbf{x}_n,\theta$ are mutually exclusive, it follows that $\mathrm{P}r\left(\Gamma_i=0,|\mathbf{x}_n,\theta\right)=1-\mathrm{P}r\left(\Gamma_i=1,|\mathbf{x}_n,\theta\right)$.

REFERENCES

[1] J. Gubbi, R. Buyya, S. Marusic, and M. Palaniswami, "Internet of things (iot): A vision, architectural elements, and future directions," *Future Generation Computer Systems*, vol. 29, no. 7, pp. 1645–1660, 2013.

[2] O. Vermesan, P. Friess, P. Guillemin, S. Gusmeroli, H. Sundmaeker, A. Bassi, I. S. Jubert, M. Mazura, M. Harrison, M. Eisenhauer *et al.*, "Internet of things strategic research roadmap," *O. Vermesan, P. Friess, P. Guillemin, S. Gusmeroli, H. Sundmaeker, A. Bassi, et al., Internet of Things: Global Technological and Societal Trends*, vol. 1, pp. 9–52, 2011.

[3] D. Bandyopadhyay and J. Sen, "Internet of things: Applications and challenges in technology and standardization," *Wireless Personal Communications*, vol. 58, no. 1, pp. 49–69, 2011.

[4] D. Miorandi, S. Sicari, F. De Pellegrini, and I. Chlamtac, "Internet of things: Vision, applications and research challenges," *Ad Hoc Networks*, vol. 10, no. 7, pp. 1497–1516, 2012.

[5] E. Arias-de Reyna and P. M. Djuric, "Indoor localization with range-based measurements and little prior information," *IEEE Sensors Journal*, vol. 13, no. 5, pp. 1979–1987, 2013.

[6] J. C. Adams, W. Gregorwich, L. Capots, and D. Liccardo, "Ultra-wideband for navigation and communications," in *Aerospace Conference, 2001, IEEE Proceedings.*, vol. 2. IEEE, 2001, pp. 2–785.

[7] C.-C. Chong, F. Watanabe, and H. Inamura, "Potential of uwb technology for the next generation wireless communications," in *2006 IEEE Ninth International Symposium on Spread Spectrum Techniques and Applications,*. IEEE, 2006, pp. 422–429.

[8] I. Guvenc and Z. Sahinoglu, "Threshold-based toa estimation for impulse radio uwb systems," in *2005 IEEE International Conference on Ultra-Wideband, 2005. ICU 2005.* IEEE, 2005, pp. 420–425.

[9] Z. A. lu, S. Gezici, and G. Ismail, *Ultra-Wideband Positioning Systems: Theoretical Limits, Ranging Algorithms, and Protocols*. Cambridge University Press, 2008.

[10] Y. Wang, X. Ma, and G. Leus, "Robust time-based localization for asynchronous networks," *IEEE Transactions on Signal Processing,*, vol. 59, no. 9, pp. 4397–4410, 2011.

[11] M. L. Sichitiu and V. Ramadurai, "Localization of wireless sensor networks with a mobile beacon," in *2004 IEEE International Conference on Mobile Ad-hoc and Sensor Systems,*. IEEE, 2004, pp. 174–183.

[12] I. Amundson and X. D. Koutsoukos, "A survey on localization for mobile wireless sensor networks," in *Mobile Entity Localization and Tracking in GPS-less Environnments*. Springer, 2009, pp. 235–254.

[13] S. G. Nagarajan, P. Zhang, and I. Nevat, "Geo-spatial location estimation for internet of things (iot) networks with one-way time-of-arrival via stochastic censoring," *IEEE Internet of Things Journal*, vol. 4, no. 1, pp. 205–214, 2017.

[14] I. Nevat, G. W. Peters, K. Avnit, F. Septier, and L. Clavier, "Location of things: Geospatial tagging for iot using time-of-arrival," *IEEE Transactions on Signal and Information Processing over Networks*, vol. 2, no. 2, pp. 174–185, 2016.

[15] Y.-C. Wu, Q. Chaudhari, and E. Serpedin, "Clock synchronization of wireless sensor networks," *IEEE Signal Processing Magazine*, vol. 28, no. 1, pp. 124–138, 2011.

[16] F. Erlacher, B. Weber, J.-T. Fischer, and F. Dressler, "Avarange-using sensor network ranging techniques to explore the dynamics of avalanches," in *2016 12th Annual Conference on Wireless On-demand Network Systems and Services (WONS)*. IEEE, 2016, pp. 1–4.

[17] "Aps011 application note: Sources of error in dw1000 based two-way ranging (twr) schemes," Tech. Rep., 2014. [Online]. Available: http://www.decawave.com/sites/default/files/resources/aps011_sources_of_error_in_twr.pdf

[18] P.-T. De Boer, D. P. Kroese, S. Mannor, and R. Y. Rubinstein, "A tutorial on the cross-entropy method," *Annals of operations research*, vol. 134, no. 1, pp. 19–67, 2005.

ISBN 978-90-827970-1-5 © EURASIP 2018